Analytical and Bioanalytical Chemistry
https://doi.org/10.1007/s00216-026-06312-9

COMMUNICATION

Tackling matrix effects in biosensor-based analysis of untreated blood plasma

Giusy Finocchiaro[1] · Markéta Bocková[1] · Jiří Homola[1]

Received: 25 October 2025 / Revised: 20 December 2025 / Accepted: 5 January 2026

Abstract
Human blood plasma is the matrix of choice for clinical diagnostic applications. However, matrix effects associated with its complex composition interfere with the accurate detection of biomarkers that are often present at extremely low concentrations. This study investigates such matrix effects, particularly the nonspecific adsorption of blood plasma to the sensor surface and the interaction of endogenous antibodies with the used receptors, and shows how they can be discriminated using a surface plasmon resonance biosensor. Moreover, we describe a strategy to tackle matrix effects by combining sequential blood plasma/buffer injections, single-surface referencing, and the addition of an antibody against endogenous immunoglobulins to blood plasma. Finally, we apply this strategy to the detection of the cancer biomarker carcinoembryonic antigen in undiluted blood plasma, achieving detection limits of 12 ng/mL using direct detection, and 225 pg/mL using a sandwich assay with functional gold nanoparticles.

Keywords Biosensor-based analysis · Surface plasmon resonance · Matrix effects · Human blood plasma

Introduction

Human blood plasma is a complex biological matrix that contains a broad spectrum of biomarkers and represents the medium of choice for clinical diagnostics. However, the most abundant blood plasma components, which are present at levels vastly exceeding those of biomarkers, produce matrix effects that interfere with analytical measurements [1]. Matrix effects represent a major concern not only for conventional analytical methods and immunoassays, such as enzyme-linked immunosorbent assays (ELISA), but also for biosensing technologies, such as surface plasmon resonance (SPR) biosensors [2, 3]. The matrix effects that impair the antibody-based detection of protein biomarkers with SPR biosensors include (i) the fouling or nonspecific adsorption (NSA) of blood plasma components to the sensor surface [1] and (ii) the interference of endogenous antibodies (hereafter referred to as interfering antibodies, IAbs) with the used receptors [4, 5].

Various approaches have been proposed to suppress the effects of NSA in SPR biosensors, such as sample treatment (i.e., dilution, filtration, or depletion of the most abundant components) [1, 6], functionalization of biosensors [7–10] and functional nanoparticles [11–13] with low-fouling coatings, and advanced detection methodologies and assay schemes [6, 14–16]. The latter includes the use of referencing approaches to compensate for the NSA contribution to the sensor response, such as the single-surface referencing (SSR) method [15], and the implementation of microfluidic approaches for washing weakly adsorbed components from the sensor surface, such as the sequential injection method [16]. However, none of these approaches address the interfering effects associated with the interaction of the IAbs with the receptors, which are typically neglected or improperly referred to as NSA in most biosensor-based analytical studies [2, 6]. Moreover, although a few investigations have reported biomarker detection in untreated biological matrices [17–21], the majority of these approaches have been demonstrated to work well only for biomarker detection in diluted biological matrices.

Published in the topical collection honoring Günter Gauglitz's lifetime achievements.

✉ Jiří Homola
homola@ufe.cz

[1] Institute of Photonics and Electronics of the Czech Academy of Sciences, Chaberská 1014/57, 182 00 Prague, Czech Republic

Published online: 19 January 2026

In this study, we show how the NSA and IAb interference can be discriminated using an SPR biosensor. We combine the SSR and sequential injection approaches to mitigate the effects of NSA, and the use of an antibody against immunoglobulin G (Ab_{IgG}) to minimize the effects associated with the IAbs. Applying this strategy, we demonstrate the detection of carcinoembryonic antigen (CEA), a biomarker associated with the progression of multiple cancer types [22], in untreated blood plasma samples.

Materials and methods

Blood plasma

Human blood samples were collected at the Institute of Hematology and Blood Transfusion (Prague, Czech Republic) in compliance with the ethical requirements of the Declaration of Helsinki. The blood plasma was separated from human blood by centrifugation at 460 × *g* for 10 min. Ethylenediaminetetraacetic acid (EDTA) was added as an anticoagulant, and the samples were stored in EDTA-coated tubes at − 80 °C until use. To obtain a representative blood plasma sample [23], we used a pooled sample derived from a cohort of ten healthy individuals of mixed genders.

SPR biosensor and chip functionalization

The six-channel SPR biosensor with temperature stabilization used in this work was developed at the Institute of Photonics and Electronics (Prague, Czech Republic) [16]. The SPR platform is based on the Kretschmann geometry and spectral modulation. In this geometry, a polychromatic light is directed onto the SPR chip at a fixed angle. The excitation of surface plasmons generates a characteristic dip in the spectrum of reflected light. A change in the refractive index due to the binding of biomolecules to the SPR chip produces a shift in the excitation wavelength, which is used as the sensor response. For the developed SPR platform, a sensor response (wavelength change) of 1 nm corresponds to a protein surface density of 17 ng/cm^2 (for details, see Supplementary information, SI).

The SPR chip was prepared by depositing 1.5 nm of titanium and 50 nm of gold on a glass substrate using electron-beam evaporation in vacuum. Prior to each biosensing experiment, the SPR chip was incubated overnight with a mixture of carboxy- and hydroxy-terminated alkanethiols at a total concentration of 200 µM in a 3:7 molar ratio. The carboxylic groups were activated on the SPR platform using 25 mM N-hydroxysuccinimide (NHS) and 95.3 mM 1-ethyl-3-(3-dimethylaminopropyl)-carbodiimide hydrochloride (EDC) for 10 min at a flow rate of 5 µL/min. Then, the primary antibody against CEA ($Ab_{1,CEA}$) was diluted in 10 mM sodium acetate (SA_{10}) to a final concentration of 10 µg/mL and flowed over the SPR chip at 20 µL/min to saturation, followed by a 2-min washing with high ionic strength phosphate buffer (PBS_{NaCl}). The surface was then passivated with 100 µg/mL bovine serum albumin (BSA) in SA_{10} at 20 µL/min to saturation, followed by PBS_{NaCl} and 0.5 M ethanolamine injections for 5 min. All buffers and reagents, along with their suppliers, are reported in Tables S1 and S2 in SI.

Approach

Herein, we combined the sequential blood plasma injection approach with the SSR method. The sequential injection approach involves alternating injections of blood plasma and a high ionic strength buffer to wash weakly adsorbed components from the sensor surface [16]. We used a dispersionless microfluidic system (Fig. S1a) with two peristaltic pumps and PBS_{NaCl} with 250 µg/mL BSA ($PBS_{NaCl + BSA}$) as the washing buffer. The blood plasma sample was injected eleven times for 30 s, each injection followed by a washing step with a duration of 30 s, both performed at a flow rate of 20 µL/min. The sensorgrams illustrating the sequential injection approach are provided in Figs. S1b and S1c; the sensorgrams in Fig. S2 demonstrate that the used washing buffer did not disrupt the specific CEA–$Ab_{1,CEA}$ interaction.

The SSR approach implies compensating for the NSA contribution to the blood plasma sensor response by using a reference channel that presents the same surface functionalization as the detection channel [15]. Specifically, a three-channel configuration was employed, involving one detection channel (spiked with a defined concentration of CEA) and two reference channels (bare blood plasma and blood plasma spiked with $Ab_{1,CEA}$). Comparison of these channels enabled the determination of the natural, spiked, and total CEA concentrations, as well as the assessment of the influence of endogenous antibodies. No treatment or dilution of the blood plasma sample was performed, except for the addition of the above-mentioned reagents (i.e., buffer with spiked CEA, $Ab_{1,CEA}$, or Ab_{IgG}), which constituted only 3% of the total sample volume.

Experimental

To establish the calibration curves for the detection of CEA in blood plasma, we measured the reference-compensated sensor response to concentrations of 50, 100, 200, 300, 500, and 1000 ng/mL CEA spiked in blood plasma. In addition to the direct detection, we performed a sandwich assay with a biotinylated secondary antibody against CEA (b-$Ab_{2,CEA}$) and streptavidin-coated gold nanoparticles (AuNPs, see SI for their preparation). The b-$Ab_{2,CEA}$ was diluted to a concentration of 10 µg/mL in phosphate buffer supplemented with 0.01% Tween 20 (PBS_{Tween}) and injected for 15 min at

10 µL/min. The AuNPs were diluted in PBS_{Tween} to a concentration of 25 pM and flowed over the sensor surface for 60 min at 5 µL/min. The same protocol was used to establish the calibration curves for the detection of CEA in blood plasma with added Ab_{IgG} (10 µg/mL). In these experiments, we measured the reference-compensated sensor response to 0.3, 1, 3, 6, 10, 15, 20, 50, 100, 200, 300, 500, and 1000 ng/mL CEA spiked in blood plasma, both with and without the enhancement due to AuNPs. The calibration curves for the direct detection of CEA were created by plotting the reference-compensated sensor response to blood plasma taken 10 min after the last buffer injection. The calibration curves for the AuNP-enhanced detection of CEA were created by plotting the reference-compensated sensor response to the AuNPs taken 5 min after the buffer injection. For comparison, the level of naturally occurring CEA in blood plasma was measured using a commercial ELISA kit from Abbott Diagnostics, USA.

Results and discussion

The approach used for CEA detection is illustrated in Fig. 1a and b, showing the sensor response to undiluted blood plasma with and without Ab_{IgG} addition. In both scenarios, Ch #1 provides the sensor response to blood plasma spiked with 300 ng/mL CEA, Ch #2 provides the sensor response to blood plasma, and Ch #3 (reference channel) provides the sensor response to blood plasma spiked with $Ab_{1,CEA}$. Figure 1a reveals a minor difference in sensor response between Ch #2 and Ch #3, which may be attributed to the naturally occurring CEA in blood plasma; whereas Fig. 1b shows a substantial difference between Ch #2 and Ch #3, suggesting a strong interfering effect associated with endogenous IAbs. Overall, Fig. 1a and b indicate that the addition of Ab_{IgG} to blood plasma significantly reduced the influence of IAbs (sensor response difference between Ch #2 and Ch #3), while it had a negligible impact on the NSA (Ch #3) and on the specific binding of CEA spiked in blood plasma (sensor response difference between Ch #1 and Ch #2). To further examine the effect of IAbs, we performed an SPR experiment using the same blood plasma sample that was depleted of the most abundant proteins (i.e., human serum albumin and IgG). In this experiment, only a negligible sensor response difference between Ch #2 and Ch #3 was observed following depletion (Fig. S3), suggesting that the sensor response to untreated blood plasma was mainly due to endogenous abundant proteins rather than naturally occurring CEA. The role of Ab_{IgG} was further explored in experiments using the SPR biosensor for the detection of two other analytes, human chorionic gonadotropin and horseradish peroxidase (Fig. S4), as well as for the detection of CEA in another blood plasma sample (Fig. S5). The

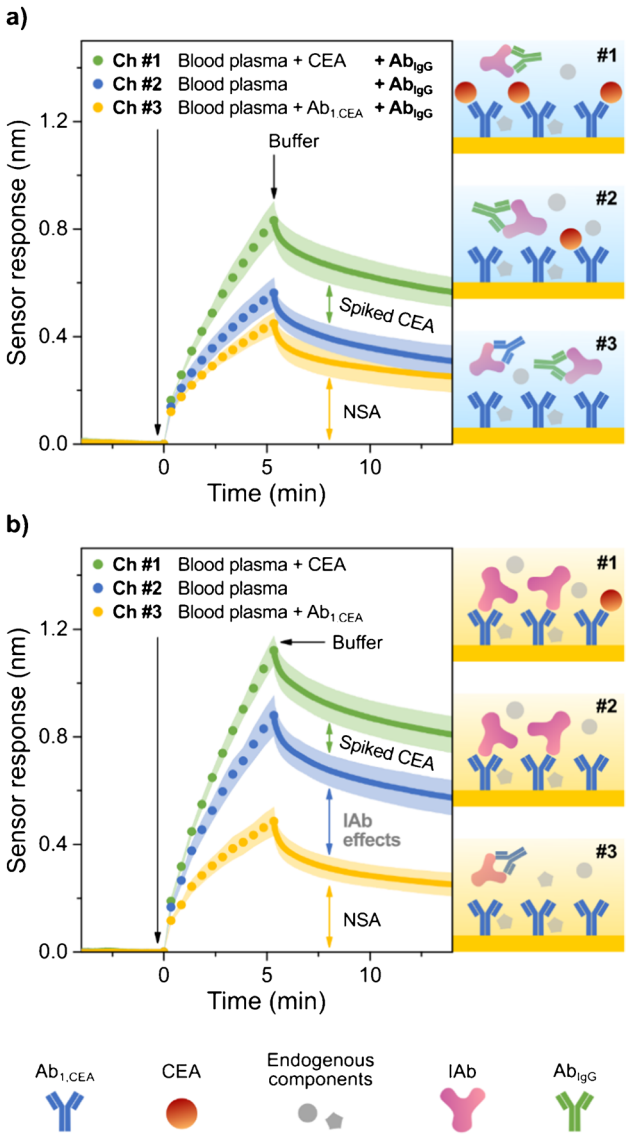

Fig. 1 Average sensor response to the binding of blood plasma spiked with 300 ng/mL CEA (Ch #1), blood plasma alone (Ch #2), and blood plasma spiked with $Ab_{1,CEA}$ (Ch #3), after adding Ab_{IgG} to the blood plasma sample (**a**), and without Ab_{IgG} addition (**b**). The shaded areas correspond to the standard deviations of at least three measurements. The panels on the right side illustrate the interactions occurring in Ch #1, Ch #2, and Ch #3 (the legend of symbols is displayed in the panel below)

results confirmed that adding Ab_{IgG} to blood plasma (independently of the analyte and sample) reduced the sensor response difference between Ch #2 and Ch #3, and thus, the effects associated with IAbs.

We measured the sensor response as a function of CEA concentration with and without Ab_{IgG} addition to blood plasma for both direct detection and AuNP-enhanced detection (Fig. 2a and b). Each data point represents the average of at least three independent measurements, with the error bars indicating the standard deviations of the individual

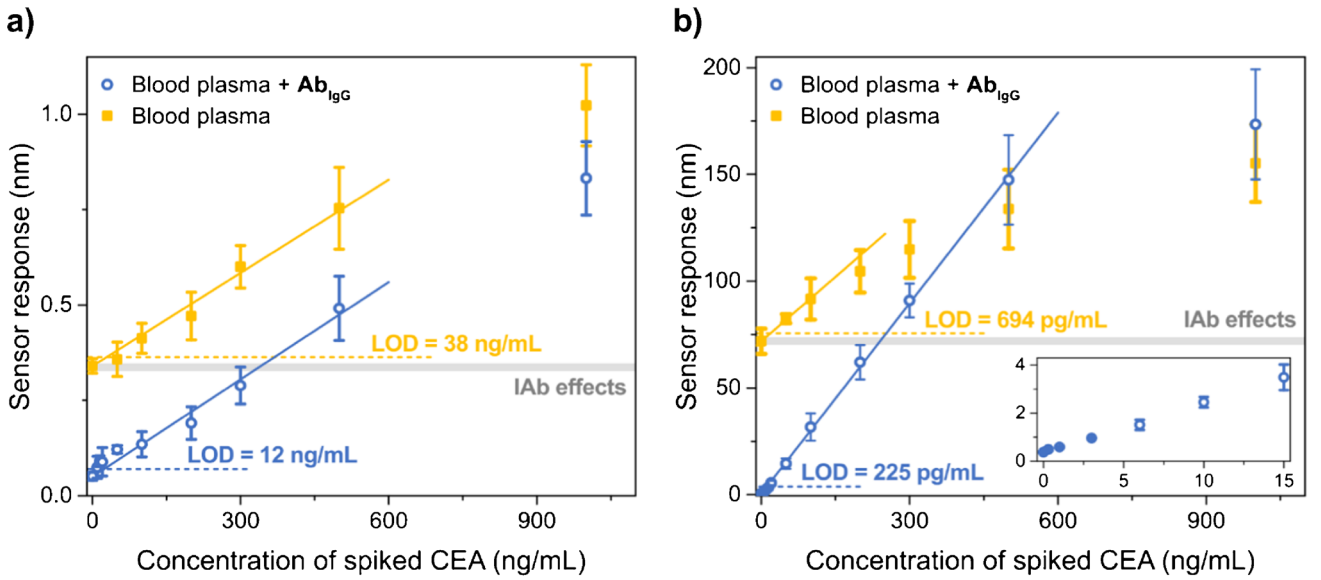

Fig. 2 Calibration curves for the detection of CEA in blood plasma with and without Ab_{IgG} addition (blue and yellow scatter, respectively), using direct detection (**a**) and a sandwich assay with AuNPs (**b**). The solid lines indicate the linear fits of the data points, and the error bars represent the standard deviations of at least three measurements. The inset in **b** shows the reference-compensated sensor response to low CEA concentrations spiked in blood plasma

measurements. The standard deviation typically fell within 10–15% of the sensor response. The offsets of the calibration curves for CEA detection in blood plasma without the addition of Ab_{IgG} (gray horizontal lines in Fig. 2a and b) were mainly associated with the interaction of IAbs with $Ab_{1,CEA}$ immobilized on the sensor surface. The sensor response to the limit of detection (LOD) was calculated from the standard deviation of at least 13 replicates of the blank measurement (Ch #3), by applying the Student's *t*-distribution with a confidence interval of 97.5% (for details, see SI). The resulting LODs suggest that the addition of Ab_{IgG} to blood plasma improves the LOD for CEA direct detection by a factor of ~ 3, while reducing the offset of the calibration curve by approximately one order of magnitude (Table S3 in SI). The achieved LOD of 12 ng/mL represents an improvement over previously reported LOD values for CEA direct detection with SPR, namely 30 ng/mL in 50% blood plasma [24] and 76 ng/mL in undiluted blood serum [18]. To enable the detection of CEA in untreated blood plasma at physiological concentrations (i.e., below 3 ng/mL [22]), a sandwich assay with AuNPs was performed (Fig. 2b). While the calibration curve for blood plasma with the addition of Ab_{IgG} starts approximately at zero for the sample not spiked with CEA, the calibration curve obtained when no Ab_{IgG} was added to blood plasma is offset by about 72 nm. These results indicate that the functional AuNPs were also binding to IAbs captured at the sensor surface. The sensor response was enhanced by the AuNPs by a factor of about 300 and 210 for blood plasma with and without Ab_{IgG} addition (estimated from the linear ranges of the calibration curves). The LODs determined for CEA detection in blood plasma with and without Ab_{IgG} were 225 pg/mL and 694 pg/mL, respectively. The LOD obtained with the presented methodology (225 pg/mL) is tenfold below the physiological threshold and is comparable to previously reported LODs for AuNP-enhanced SPR-based detection in 50% blood plasma [12, 24, 25] or in 0.1% blood serum [26]. It should be noted that the offset of 0.37 nm observed at zero concentration of CEA in blood plasma after Ab_{IgG} addition (inset in Fig. 2b) corresponds to a concentration of naturally occurring CEA of 1.2 ng/mL, which was in excellent agreement with the value determined by ELISA (1.7 ng/mL). The presented strategy enabled the detection of CEA over a dynamic range spanning 3 orders of magnitude, from the lowest measured concentration of 0.3 ng/mL to the concentration of 500 ng/mL CEA, which approaches the highest CEA concentrations observed at pathological conditions [27].

Conclusions

We investigate and discriminate between blood plasma matrix effects, particularly the nonspecific adsorption to the sensor surface and the interaction of endogenous antibodies (IAbs) with the receptor, using an SPR biosensor. We combine the sequential injection and single-surface referencing approaches to mitigate the nonspecific adsorption,

along with Ab_{IgG} to reduce the effects associated with IAbs. We apply this strategy to the detection of CEA in undiluted blood plasma using an SPR biosensor, demonstrating a reduction of IAb effects by a factor of 10 when using direct detection and nearly 200 when using a sandwich assay with AuNP enhancement. The approach enables CEA direct detection in undiluted blood plasma at levels as low as 12 ng/mL, representing the best LOD achieved by an SPR biosensor for CEA direct detection in blood plasma or serum. In conjunction with the sandwich assay, the proposed strategy yields an LOD of 225 pg/mL, which is an order of magnitude below the physiological threshold. This suggests that the proposed methodology enables the robust detection of clinically relevant levels of CEA in untreated blood plasma samples. This approach can potentially be adapted to a broad range of protein biomarkers and biological matrices. The benefits are expected to depend on the composition of the biological matrix, particularly on the concentration of IAbs; higher performance improvement may be expected in matrices with higher IAb levels.

Supplementary Information The online version contains supplementary material available at https://doi.org/10.1007/s00216-026-06312-9.

Acknowledgements The authors are grateful to Dr. Leona Chrastinová and Dr. Ondřej Pastva for providing the blood plasma samples used in this study, and to Coline Moutard for her help in functionalizing the AuNPs. The illustrations in this article were created with Inkscape.

Author contribution GF: conceptualization, methodology, writing—original draft; MB: supervision, methodology, writing—review and editing; JH: supervision, funding acquisition, writing—review and editing.

Funding This research was supported by the National Institute for Cancer Research (contract LX22NPO5102) and by the Czech Science Foundation (contract 20–23787X).

Data availability The data are available at the link https://doi.org/10.5281/zenodo.17340883.

Declarations

Ethics approval The blood samples were obtained in compliance with the regulations outlined in the Declaration of Helsinki, under the approval of the Ethics Committee of the Institute of Hematology and Blood Transfusion. All the study participants signed an informed consent at the time of blood collection.

Conflict of interest The authors declare no competing interests.

References

1. Frutiger A, Tanno A, Hwu S, Tiefenauer RF, Voros J, Nakatsuka N. Nonspecific binding-fundamental concepts and consequences for biosensing applications. Chem Rev. 2021;121(13):8095–160.
2. Masson JF. Surface plasmon resonance clinical biosensors for medical diagnostics. ACS Sens. 2017;2(1):16–30.
3. Špringer T, Bocková M, Slabý J, Sohrabi F, Čapková M, Homola J. Surface plasmon resonance biosensors and their medical applications. Biosens Bioelectron. 2025;278: 117308.
4. Kricka LJ. Human anti-animal antibody interferences in immunological assays. Clin Chem. 1999;45(7):942–56.
5. Bjerner J, Olsen KH, Børmer OP, Nustad K. Human heterophilic antibodies display specificity for murine IgG subclasses. Clin Biochem. 2005;38(5):465–72.
6. Visentin J, Couzi L, Dromer C, Neau-Cransac M, Guidicelli G, Veniard V, Coniat KN, Merville P, Di Primo C, Taupin JL. Overcoming non-specific binding to measure the active concentration and kinetics of serum anti-HLA antibodies by surface plasmon resonance. Biosens Bioelectron. 2018;117:191–200.
7. Breault-Turcot J, Chaurand P, Masson J-F. Unravelling nonspecific adsorption of complex protein mixture on surfaces with SPR and MS. Anal Chem. 2014;86(19):9612–9.
8. D'Agata R, Bellassai N, Jungbluth V, Spoto G. Recent advances in antifouling materials for surface plasmon resonance biosensing in clinical diagnostics and food safety. Polymers. 2021;13(12):1929.
9. Wiesner F, Petri C, Hageneder S, Kunzler C, Klees S, Frank P, Pertiller M, Dostalek J, Knoll W, Jonas U. Thermoresponsive and photocrosslinkable poly (2-alkyl-2-oxazoline) toolbox–customizable ultralow-fouling hydrogel coatings for blood plasma environments. Macromol Rapid Commun. 2024;45(4):2300549.
10. Gunkel G, Weinhart M, Becherer T, Haag R, Huck WT. Effect of polymer brush architecture on antibiofouling properties. Biomacromol. 2011;12(11):4169–72.
11. Fenzl C, Genslein C, Domonkos C, Edwards K, Hirsch T, Baeumner A. Investigating non-specific binding to chemically engineered sensor surfaces using liposomes as models. Analyst. 2016;141(18):5265–73.
12. Špringer T, Homola J. Biofunctionalized gold nanoparticles for SPR-biosensor-based detection of CEA in blood plasma. Anal Bioanal Chem. 2012;404:2869–75.
13. Zhang S, Geryak R, Geldmeier J, Kim S, Tsukruk VV. Synthesis, assembly, and applications of hybrid nanostructures for biosensing. Chem Rev. 2017;117(20):12942–3038.
14. Lichtenberg JY, Ling Y, Kim S. Non-specific adsorption reduction methods in biosensing. Sensors. 2019;19(11):2488.
15. Špringer T, Bocková M, Homola J. Label-free biosensing in complex media: a referencing approach. Anal Chem. 2013;85(12):5637–40.
16. Špringer T, Piliarik M, Homola J. Real-time monitoring of biomolecular interactions in blood plasma using a surface plasmon resonance biosensor. Anal Bioanal Chem. 2010;398(5):1955–61.
17. Masson J-F, Battaglia TM, Khairallah P, Beaudoin S, Booksh KS. Quantitative measurement of cardiac markers in undiluted serum. Anal Chem. 2007;79(2):612–9.
18. Yavas O, Acimovic SS, Garcia-Guirado J, Berthelot J, Dobosz P, Sanz V, Quidant R. Self-calibrating on-chip localized surface plasmon resonance sensing for quantitative and multiplexed detection of cancer markers in human serum. ACS Sens. 2018;3(7):1376–84.

19. Vaisocherová H, Yang W, Zhang Z, Cao Z, Cheng G, Piliarik M, Homola J, Jiang S. Ultralow fouling and functionalizable surface chemistry based on a zwitterionic polymer enabling sensitive and specific protein detection in undiluted blood plasma. Anal Chem. 2008;80(20):7894–901.
20. Kotlarek D, Vorobii M, Ogieglo W, Knoll W, Rodriguez-Emmenegger C, Dostalek J. Compact grating-coupled biosensor for the analysis of thrombin. ACS Sens. 2019;4(8):2109–16.
21. Brault ND, White AD, Taylor AD, Yu Q, Jiang S. Directly functionalizable surface platform for protein arrays in undiluted human blood plasma. Anal Chem. 2013;85(3):1447–53.
22. Sun H, Liu J, Zhang Q, Yang L, Zhou M, Song D. Advances in carcinoembryonic antigen detection: a review of clinical applications and standardization. Anal Bioanal Chem. 2025;417:1751–64.
23. de los Santos Pereira A, Rodriguez-Emmenegger C, Surman F, Riedel T, Alles AB, Brynda E. Use of pooled blood plasmas in the assessment of fouling resistance. RSC Adv. 2014;4(5):2318–21.
24. Špringer T, Chadtová Song X, Ermini ML, Lamačová J, Homola J. Functional gold nanoparticles for optical affinity biosensing. Anal Bioanal Chem. 2017;409(16):4087–97.
25. Szymanska B, Lukaszewski Z, Hermanowicz-Szamatowicz K, Gorodkiewicz E. An immunosensor for the determination of carcinoembryonic antigen by surface plasmon resonance imaging. Anal Biochem. 2020;609:113964.
26. Li R, Feng F, Chen Z-Z, Bai Y-F, Guo F-F, Wu F-Y, Zhou G. Sensitive detection of carcinoembryonic antigen using surface plasmon resonance biosensor with gold nanoparticles signal amplification. Talanta. 2015;140:143–9.
27. Zhang K, Huo H, Lin G, Yue Y, Wang Q, Li J. A long way to go for the harmonization of four immunoassays for carcinoembryonic antigen. Clin Chim Acta. 2016;454:15–9.